Examine Sleep Stages Applying HOS methods, Cepstral Analysis and Machine Learning Techniques

Alexandros Tsiggilis, Georgios Papadimitriou

***Abstract*—An technique to extracting characteristics from polysomnographic sleep recordings (PSGs) suited for automated sleep assessment combining higher order statistics (HOS), cepstral analysis, principal component analysis (PCA), and machine learning. An open-source dataset is utilized, consisting of 151 PSGs (4xEEG, chin EMG,2xEOG, ECG). Features extracted from EEG,EOG, EMG and ECG using HOS, PCA, cepstral analysis and bicepstral analysis. The analysis is combined with the implementation of KNN machine learning classification model. The results demonstrate that the classification method achieves high agreement with annotators.**

***Index Terms*—Sleep Scoring, Bispectrum, Bicoherence, Cepstrum,Bicepstrum, KNN,PCA**

I. Introduction

SLEEP is a fundamental and enigmatic aspect of human life, occupying a substantial portion of our existence. It is a dynamic process comprising several distinct stages, each with its unique characteristics and functions. In recent years, the study of sleep has evolved significantly, with researchers employing innovative techniques to delve deeper into the intricacies of sleep stages. This research paper embarks on a comprehensive exploration of the five primary sleep stages: Awake, NREM1, NREM2, NREM3, and REM, while simultaneously delving into the utilization of higher-order statistics for processing patient sleep data. By merging traditional sleep stage analysis with advanced statistical methodologies, we aim to shed new light on sleep patterns and their implications for health and well-being.

The journey into the realm of sleep begins with the Awake stage. It represents the baseline of consciousness and alertness. During this stage, individuals are fully aware of their surroundings, with their senses actively processing information. Brain wave patterns exhibit high-frequency, low-amplitude beta waves, and muscle activity is optimized for physical engagement. The Awake stage serves as a critical foundation upon which the rest of the sleep cycle is built.

NREM1 is the transitional phase between wakefulness and deeper sleep. It typically lasts only a few minutes. As individuals begin to relax and close their eyes, brain wave patterns shift from beta waves to alpha waves, which are slower and more synchronized. During NREM1, individuals may experience hypnagogic hallucinations or brief, dream-like thoughts. Muscle activity starts to decrease, occasionally accompanied by hypnic jerks, sudden muscle contractions. This stage is delicate and easily disrupted.

NREM2 constitutes the majority of the sleep cycle and offers a more stable environment for rest. It is characterized by the presence of sleep spindles and K-complexes in brain wave patterns. Sleep spindles are brief bursts of brain activity, while K-complexes are large, slow waves that help protect sleepers from external stimuli. During NREM2, body temperature decreases, heart rate and breathing become more regular, and muscles continue to relax. NREM2 is crucial for consolidating memories and preparing the body for deeper sleep.

Also known as slow-wave sleep (SWS) or deep sleep, NREM3 is the most restorative stage. It features slow delta wave activity and can be difficult to awaken from. During NREM3, growth hormone is released, tissues are repaired, and the immune system receives a boost. Deep sleep is essential for feeling refreshed and alert the next day.

REM sleep is the most captivating stage, characterized by rapid eye movements and vivid dream experiences. It typically occurs about 90 minutes after falling asleep and recurs several times throughout the night, increasing in duration with each cycle. During REM sleep, brain activity becomes similar to that of wakefulness, and vivid dreams are generated. However, the body remains in a state of temporary paralysis, a protective mechanism to prevent acting out dream content. REM sleep is essential for cognitive processes like memory consolidation and emotional regulation.

A particularly helpful aspect for the identification of various sleep disorders is the length of time that each stage takes up during a session, together with information on sleep patterns. [6] Therefore, one of the most crucial jobs during the clinical analysis of polysomnographic sleep recordings (PSGs) is sleep staging. A PSG serves as the fundamental diagnostic tool for many sleep disorders, recording the pertinent biological signals of a patient in the context of sleep medicine investigations. Electroencephalography (EEG), electrooculography (EOG), electromyography (EMG), and electrocardiography (ECG) would often be available via many channels. Because each sleep stage is distinguished by a set of common physiological markers, each of these signals provides information about that state.

Traditionally, sleep stage analysis has relied on visual scoring by trained experts using data from EEG, EMG, EOG and ECG measurements. While this approach has been invaluable for understanding sleep, it is labor-intensive and subject to inter-rater variability. The detection of the different phases of sleep using EEG signals has been shown to be the most accurate method [8]; hence, a significant amount of research on automated sleep scoring has been devoted to analyzing and rating the characteristics retrieved from a single EEG channel. Despite the drawbacks of polysomnography, which have made this technology more popular over time[9], found that PSG recordings are still necessary when dealing with irregular

sleep patterns. An average PSG examination includes 8 to 24 hours of continuous signal collection, and an experienced physician typically analyzes the data manually. Due to the time commitment required from the clinicians engaged and the intricacy of the study, the scoring procedure is correspondingly costly and labor-intensive. Moreover, as the public becomes more aware of sleep problems and their detrimental effects on health, there is an increasing need for PSG studies. This desire is driven by recent clinical results. For the already overcrowded sleep facilities with their long waiting lists, this poses a dilemma. Given the potential for significant time and labor savings, the automatic study of the sleep macrostructure is intriguing. An additional benefit is the potential to provide deterministic (repeatable) diagnostic results, helping to standardize and enhance the diagnostic process.

Enter the world of higher-order statistics (HOS) signal processing methods. HOS techniques offer an innovative and powerful alternative for the analysis of sleep data. These methods extend beyond conventional spectral analysis and time-domain techniques, providing a more comprehensive and data-driven approach to understanding sleep patterns. Combined with deep learning algorithms, it is an effort to develop a reliable automated sleep scoring model based on PSG data from an open-source dataset using machine learning.

II. MATHEMATICAL ANALYSIS

A. Bispectrum

The bispectrum is a fundamental concept in signal processing and spectral analysis, particularly in the field of nonlinear signal processing. It extends the concept of the power spectrum, which characterizes the energy distribution of a signal in the frequency domain, by capturing nonlinear interactions between different frequency components. The bispectrum quantifies third-order statistics by examining the relationships among three different frequencies in a signal. It is a complex-valued function that indicates whether these frequencies exhibit phase coupling, meaning that their phases are related in a nonlinear way. When the bispectrum of a signal is non-zero at specific frequency combinations, it suggests the presence of nonlinear interactions or coupling between those frequencies.This phenomenon is called Quadratic Phase Coupling (QPC). It indicates that three frequencies in a signal are related in a quadratic manner as we mentioned above, which implies that they are not simply linearly related but exhibit more complex, nonlinear interactions. QPC is valuable in various fields, including neuroscience and physics, where it helps uncover nonlinear dependencies and synchronization patterns in data that may be missed by linear methods. It plays a crucial role in understanding complex systems and their underlying dynamics.[11] Out of all the Higher-OrderSpectra, the bispectrum is by far the most extensively utilized since it gives an easy technique to detect quadratic-phase coupling (QPC) between two frequency components of a signal. [12], [13], [14] QPC is the sum of phases at two frequency variables given by $f_1 + f_2$. Mathematically, the bispectrum $B(f_1, f_2)$ of a signal $x(t)$ is defined as follows [15]:

$$B(f_1, f_2) = E\{X(f_1)X(f_2)X^*(f_1 + f_2)\}$$

Where:

- $B(f_1, f_2)$ represents the bispectrum at frequencies f_1 and f_2.
- $X(f)$ denotes the Fourier transform of the signal $x(t)$.
- $X^*(f)$ denotes the complex conjugate of $X(f)$.
- $E\{\cdot\}$ denotes the expected value or ensemble average.

Bispectrum can be estimated by two approaches: direct and indirect methods. In this work we used the direct method, which is presented next.

Let $x(t)$ is the signal:

1) Partition $y(t)$ into K segments of M samples.

$$y^i(k), \;\; i = 0, 1, 2, ..., K, \;\; k = 0, 1, ..., M-1$$

2) Subtract the mean value from each segment.

$$x_i(k) = y^i(k) - \bar{y}^i(k)$$

3) Compute the DFT of each segment.

$$F_x^i(\lambda) = \sum_{k=0}^{M-1} x^i(k) e^{-j\frac{2\pi}{M}k\lambda}$$

4) Then we estimate the bispectrum for each segment.

$$\hat{b}_3^{x^i}(\lambda_1, \lambda_2) = \frac{1}{\Delta_0^2} F_x^i(\lambda_1) F_x^i(\lambda_2) F_x^{i\,*}(\lambda_1 + \lambda_2)$$

for every λ_1, λ_2 in the primary region $PR = \{(\lambda_1, \lambda_2) \in \mathbb{R}^2 \; : \; 0 \le \lambda_2 \le \lambda_1 \le f_s/2, \; \lambda_1 + \lambda_2 \le f_c\}$

5) The bispectrum is estimated by taking the average across the K segment estimations.

$$\hat{C}_3^x(\omega_1, \omega_2) = \frac{1}{K} \sum_{i=1}^{K} \hat{b}_3^x(\omega_1, \omega_2)$$

where $\omega_1 = \left(\frac{2\pi f_s}{N_0}\right)\lambda_1, \;\; \omega_2 = \left(\frac{2\pi f_s}{N_0}\right)\lambda_2$

B. Bicoherence

Bicoherence is a critical concept derived from the bispectrum, with a particular relevance in understanding the Quasi-Periodic Component (QPC) phenomenon in signal analysis [14]. The bispectrum, which characterizes the three-way interactions among different frequency components in a signal, plays a fundamental role in identifying nonlinearity and phase coupling. In the context of QPC, the bispectrum is a powerful tool for detecting hidden periodic or quasi-periodic behaviors within a signal.

Now, Bicoherence, a derivative of the bispectrum, takes a narrower focus. It examines the pairwise correlations within these interactions, specifically honing in on how pairs of frequency components co-modulate or co-phase together. In the realm of QPC analysis [12],[13], Bicoherence becomes instrumental in uncovering the presence and characteristics of quasi-periodic components, shedding light on their frequencies, phases, and interactions.In practice, it is more convenient to use a normalized version of the bispectrum to detect quadratic phase coupling, called the Bicoherence index. Many

methods have been proposed to normalize the bispectrum. The one used here [16] is obtained as follows:

$$\mathrm{bic}\left(f_1, f_2\right) = \frac{\left|B\left(f_1, f_2\right)\right|^2}{P\left(f_1\right) P\left(f_2\right) P\left(f_1 + f_2\right)}$$

where $B\left(f_1, f_2\right)$ is the final estimate of the bispectrum, and $P(f)$ is the final estimate of the power spectrum.

C. Cepstrum

Cepstrum is a mathematical technique used in signal processing to analyze the spectral characteristics of a signal by examining its spectrum in a unique way. It involves taking the Fourier transform of the logarithm of the magnitude of the Fourier transform of a signal, effectively emphasizing the signal's spectral envelope while suppressing fine spectral details. The resulting cepstrum represents the signal's "quefrency" domain, offering insights into features like pitch [17], timbre, and echo delay in audio signals. Cepstral analysis is widely employed in applications like speech recognition, audio processing, and image analysis, where it helps identify and extract meaningful information from complex signals. The complex cepstrum of a signal x(t) calculated as [18] :

$$c(n) = \frac{1}{2\pi} \int_{-\pi}^{\pi} log(X(\omega)) e^{i\omega}\, d\omega$$

The real cepstrum of x(t) is computed as follows:

$$r(n) = \frac{1}{2\pi} \int_{-\pi}^{\pi} log|X(\omega)| e^{i\omega}\, d\omega$$

D. Machine learning - KNN method

K-Nearest Neighbors (KNN) is a simple yet effective machine learning method used for classification and regression tasks. In KNN, when predicting the class or value of a data point, it looks at the K nearest data points in the training dataset, based on a chosen distance metric (e.g., Euclidean distance) [36]. It then assigns the most common class (for classification) or averages the values (for regression) among those K neighbors to make the prediction. KNN is non-parametric and lazy, meaning it doesn't learn a model but stores the entire training data for predictions. Its flexibility and ease of implementation make it valuable for various applications.The mathematical background for KNN-method [37],[38], follows:

Suppose we have pairs $\left(X_1, Y_1\right), \left(X_2, Y_2\right), \ldots, \left(X_n, Y_n\right)$ taking values in $\mathbb{R}^d \times \{1, 2\}$, where Y is the class label of X, so that $X \mid Y = r \sim P_r$ for $r = 1, 2$ (and probability distributions P_r). Given some norm $\|\cdot\|$ on $\mathbb{R}^d$ and a point $x \in \mathbb{R}^d$, let $\left(X_{(1)}, Y_{(1)}\right), \ldots, \left(X_{(n)}, Y_{(n)}\right)$ be a reordering of the training data such that $\left\|X_{(1)} - x\right\| \leq \cdots \leq \left\|X_{(n)} - x\right\|$.

E. Bicepstrum

Bicepstrum is an alternative approach for calculating cepstral coefficients using the area of the bispectrum.In particular, Bicepstral analysis is an extension of the well-known cepstral analysis, which has been widely used in signal processing and feature extraction tasks. While cepstral analysis provides a means to represent signals in the frequency domain, bicepstral analysis takes this a step further by considering the interactions between different frequency components in the signal. In essence, bicepstral analysis explores the second-order relationships between spectral components, offering a richer representation of the signal's characteristics. The bicepstral coefficients capture nonlinear interactions in the signal, making them a valuable tool for detecting nonlinearity in various applications, including sleep stage classification. By focusing on these higher-order spectral interactions, bicepstral analysis allows us to extract features that might be missed by traditional linear methods. In addition, for obtaining the cepstral coefficients from the bicepstral coefficients, the key is that we carry out our findings via the third-order cumulants without utilizing any phase unwrapping approach. Moreover, the use of third-order cumulants provides the advantage of a noise-free space. There are two ways to calculate bicepstrum [16]. The first is to consider the transfer function $H(Z)$ of a LTI system and the corresponding bispectrum given for a signal $x(t)$ by

$$C_3^X(z_1, z_2) = \frac{\gamma_3^w A^3}{2\pi^2} H(z_1) H(z_2) H(z_1^{-1} z_2^{-1})$$

that is similar to

$$C_3^X(z_1, z_2) = \sum_{\tau_1=-\infty}^{\infty} \sum_{\tau_2=-\infty}^{\infty} c_3^x(z_1, z_2) z_1^{-\tau_1} z_2^{-\tau_2}$$

Taking the logarithm of the bispectrum we get :

$$\begin{aligned} B_x\left(z_1, z_2\right) = \log[C_3^x\left(z_1, z_2\right)] & \\ = \log|C| + \log\left[I\left(z_1^{-1}\right)\right] & \\ + \log\left[I\left(z_2^{-1}\right)\right] + \log\left[I\left(z_1 z_2\right)\right] & \\ + \log\left[O\left(z_1\right)\right] + \log\left[O\left(z_2\right)\right] & \\ + \log\left[O\left(z_1^{-1} z_2^{-1}\right)\right] & \end{aligned}$$

The bicepstrum is obtained by taking the 2D-IZT transform:

$$b_x(m,n) = \begin{cases} \log|C|, & m = 0, n = 0 \\ -\frac{1}{n} A^{(n)}, & m = 0, n > 0 \\ -\frac{1}{m} A^{(m)}, & m > 0, n = 0 \\ \frac{1}{m} B^{(-m)}, & m < 0, n = 0 \\ -\frac{1}{n} B^{(-n)}, & m = 0, n < 0 \\ -\frac{1}{n} B^{(n),} & m = n > 0 \\ \frac{1}{n} A^{(-n)}, & m = n < 0 \\ 0, & \text{otherwise} \end{cases},$$

where $A^{(k)}$ and $B^{(k)}$ correspond to the cepstral parameters

$$A^{(k)} = \sum_{i=1}^{L_1} a_i^k - \sum_{i=1}^{L_3} c_i^k,$$

$$B^{(k)} = \sum_{i=1}^{L_2} b_i^k.$$

Because $B_x(z_1, z_2)$ is analytic in its region of convergence (containing the unit circle) it is possible to compute the partial differential with regard to z_1 or z_2

$$\begin{aligned}\frac{\partial B_x(z_1,z_2)}{\partial z_1} &= \frac{1}{C_3^x(z_1,z_2)}\frac{\partial C_3^x(z_1,z_2)}{\partial z_1} \\ &\Leftrightarrow C_3^x(z_1,z_2)\, z_1 \frac{\partial B_x(z_1,z_2)}{\partial z_1} \\ &= z_1 \frac{\partial C_3^x(z_1,z_2)}{\partial z_1}.\end{aligned}$$

from above a linear convolution is implied, that is

$$c_3^x(m,n) * [-m b_x(m,n)] = -m c_3^x(m,n).$$

If we substitute the $b_x(m,n)$ we get the cepstral equation

$$\begin{aligned}\sum_{k=1}^{\infty} \Big\{ A^{(k)} &\left[c_3^x(m- \ k,n) - c_3^x(m+k,n+k)\right] \\ &+B^{(k)}\left[c_3^x(m-k,n-k) - c_3^x(m+k,n)\right]\Big\} \\ &= -m c_3^x(m,n).\end{aligned}$$

It is observed that the cepstral coefficients $A^{(k)}$ and $B^{(k)}$ are directly connected with the third-order cumulants.

As $|a_i| < 1, |c_i| < 1$ and $|b_i| < 1$ for all i, the above equation could be truncated to the approximated cepstral equation

$$\begin{aligned}\sum_{i=1}^{p} A^{(i)} &\left[c_3^x(m- \ i,n) - c_3^x(m+i,n+i)\right] \\ &+ \sum_{j=1}^{q} B^{(j)}\left[c_3^x(m-j,n-j) - c_3^x(m+j,n)\right] \\ &\cong -m c_3^x(m,n).\end{aligned}$$

The integers p, q could be selected as

$$p = \ln c / \ln a, q = \ln c / \ln b,$$

with $\max\left[|a_i|, |c_i|\right] < a < 1, \max\left[|b_i|\right] < b < 1$, and c is a very small constant (e.g., 10^{-4}), so $A^{(k)} = 0$ for $k > p$ and $B^{(k)} = 0$ for $k > q$; apparently we need to have an a priori knowledge about the pole-zero location of $H(z)$.

The second method for bicepstrum estimation based on 2D-FFT and inverse 2D-FFT (2D-IFFT) [16]. It can be calculated as follows :

$$b_x(m,n) = \frac{1}{m} 2\mathrm{D} - \mathrm{IFFT}\left\{\frac{2\mathrm{D} - \mathrm{FFT}\left[m c_3^x(m,n)\right]}{2\mathrm{D} - \mathrm{FFT}\left[c_3^x(m,n)\right]}\right\}.$$

with the size of the region of support of $2\mathrm{D}-\mathrm{I/FFT}$ be chosen $\geq 2\max\{p,q\}$.The approach of estimating the $b_x(m,n)$ based on the second method instead of the first is more attractive when the values of p and q are quite large.

F. PCA

Principal Component Analysis (PCA) is a powerful dimensionality reduction technique widely used in data analysis and feature extraction [35]. In our journal paper, we employ PCA to reduce the complexity of high-dimensional data, such as EEG signals in sleep studies. By finding the principal components that maximize data variance, PCA allows us to retain essential information while reducing noise. This not only enhances data visualization but also improves predictive modeling, aiding in tasks like sleep stage classification. PCA provides a rigorous mathematical framework to simplify and interpret complex data, making it a valuable tool in our research for insightful and efficient data analysis. Mathematically PCA is described as an orthogonal linear transformation that relocates the data to a new coordinate system such that the largest variance by some scalar projection of the data ends up being on the first coordinate (referred to as the first principal component), the second greatest variance on the second coordinate, and so on. Consider a $n \times p$ data matrix, X, with a column-wise empirical mean of zero (the sample mean of each column has been shifted to zero), where each of the n rows corresponds to a different iteration of the experiment and each of the p columns provides a specific type of feature (for example, the readings from a specific sensor). In particular, the transformation is defined by a set of size l of p-dimensional vectors of weights or coefficients $\mathbf{w}_{(k)} = (w_1, \ldots, w_p)_{(k)}$ that map each row vector $\mathbf{x}_{(i)}$ of $\mathbf{X}$ to a new vector of principal component scores $\mathbf{t}_{(i)} = (t_1, \ldots, t_i)_{(i)}$ [33],[34],[35], given by

$$t_{k(i)} = \mathbf{x}_{(i)} \cdot \mathbf{w}_{(k)} \quad \text{for} \quad i = 1, \ldots, n \quad k = 1, \ldots, l$$

in such a way that the individual variables $t_1, \ldots, t_l$ of $\mathbf{t}$ considered over the data set successively inherit the maximum possible variance from $\mathbf{X}$, with each coefficient vector $\mathbf{w}$ constrained to be a unit vector (where l is usually selected to be strictly less than p to reduce dimensionality). The k-th component can be found by subtracting the first $k-1$ principal components from $\mathbf{X}$:

$$\hat{\mathbf{X}}_k = \mathbf{X} - \sum_{s=1}^{k-1} \mathbf{X}\mathbf{w}_{(s)}\mathbf{w}_{(s)}^{\top}$$

and then finding the weight vector which extracts the maximum variance from this new data matrix

$$\mathbf{w}_{(k)} = \underset{\|\mathbf{w}\|=1}{\arg\max}\left\{\left\|\hat{\mathbf{X}}_k\mathbf{w}\right\|^2\right\} = \arg\max\left\{\frac{\mathbf{w}^{\top}\hat{\mathbf{X}}_k^{\top}\hat{\mathbf{X}}_k\mathbf{w}}{\mathbf{w}^T\mathbf{w}}\right\}$$

It turns out that this gives the remaining eigenvectors of $\mathbf{X}^{\top}\mathbf{X}$, with the maximum values for the quantity in brackets given by their corresponding eigenvalues. Thus the weight vectors are eigenvectors of $\mathbf{X}^{\top}\mathbf{X}$. The k-th principal component of a data vector $\mathbf{x}_{(i)}$ can therefore be given as a score $t_{k(i)} = \mathbf{x}_{(i)} \cdot \mathbf{w}_{(k)}$ in the transformed coordinates, or as the corresponding vector in the space of the original variables, $\left\{\mathbf{x}_{(i)} \cdot \mathbf{w}_{(k)}\right\}\mathbf{w}_{(k)}$, where $\mathbf{w}_{(k)}$ is the k th eigenvector of $\mathbf{X}^{\top}\mathbf{X}$. The full principal components decomposition of $\mathbf{X}$ can therefore be given as

$$\mathbf{T} = \mathbf{X}\mathbf{W}$$

where $\mathbf{W}$ is a p-by-p matrix of weights whose columns are the eigenvectors of $\mathbf{X}^{\top}\mathbf{X}$. The transpose of $\mathbf{W}$ is sometimes called the whitening or sphering transformation. Columns of $\mathbf{W}$ multiplied by the square root of corresponding eigenvalues, that is, eigenvectors scaled up by the variances, are called loadings in PCA or in Factor analysis.

III. Materials and Methods

A. Dataset

We took patient data from the Haaglanden Medisch Centrum sleep staging database, which is an open database in physionet [22] and contains 151 (whole-night polysomnographic (PSG)) sleep recordings (85 males and 66 females, with a mean age of 53.9 15.4) collected in 2018 at the Haaglanden Medisch Centrum (HMC, The Netherlands) sleep center. Four EEG channels (F4/M1, C4/M1, O2/M1, and C3/M2), two EOG channels (E1/M2 and E2/M2), one bipolar chin EMG, and one ECG are all included in the PSG recordings. The dataset contains the associated hypnogram annotations in addition to the recordings. The AASM recommendations from version 2.4 state that every 30 seconds of sleep should be accompanied with an annotation. The sampling frequency for all signals were 256Hz. Using AgAgCl electrodes, signals were captured with SOMNOscreen PSG, PSG+, and EEG recorders. Records from a diverse population that was referred for a PSG evaluation in the context of various sleep disorders were chosen at random. However, the annotated data for these illnesses has not been made available.

B. Data Preparation

The PSG recordings where sampled and digitized with sampling frequency $f_s = 256Hz$. With the help of human annotation segment of duration 30 seconds were annotated and assign a sleep stage. Every such 30-second segment is called an epoch. Every epoch consist of 8 digital signals with 7680 samples, each one corresponding to a different channel of the recording.

C. Cepstral analysis

This paper applies cepstral analysis for periodic structures detection and impulse response estimation across to the polysomnographic sleep recordings for all of the patients. Our main objective while performing cepstral analysis of the EEGs, EOGs, EMG and ECG channels was to represent transitions between different stages of sleep. For that reason we further produced a detailed analysis. Two methods are followed for each channel (EEG ,ECG etc.) individually in order to compute the cepstrum values .In the first method, cepstral coefficients are calculated for each patient separately along with the whole set of sleep stages recordings, and then we take the average over all of these values. We estimate also the impulse response for mixed-phase and minimum-phase cases in these derived coefficients. In the second approach, we calculate the average data vector-record of all the polysomnographic data records, which are called "epochs" for a specific channel with a distinct state of sleep for each patient. Then, we determine the cepstral coefficients and the impulse response estimates. Examining a large amount of available data for each channel, we find useful results only for EOG_E1_M2 channel using the second method as described above. Analyzing EOG_E1_M2 data, we obtain the cepstral coefficients and the impulse response estimations as illustrated in figure 1. We observe that there is a periodic prominence with quefrency t=0.15625s which associated in a frequency f=192Hz. This estimated periodicity appears for all sleep stages in EOG_E1_M2 channel. Although, as patient moves into a deeper sleep stage, we can see that this periodic prominence seems to be stronger with every change.

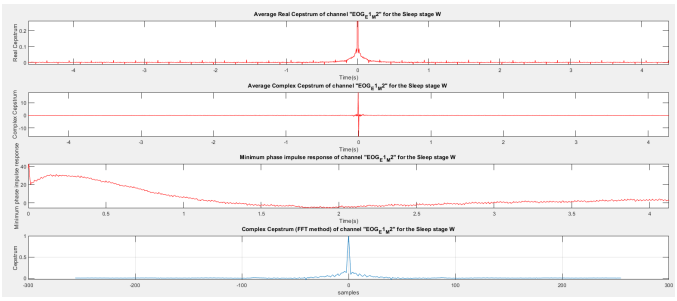

(a) Sleep stage: Weak

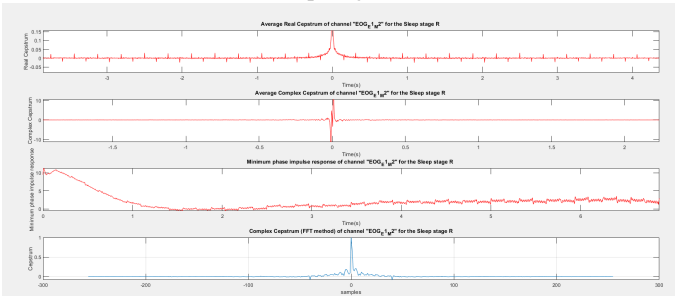

(b) Sleep stage: REM

Fig. 1: EOG_E1_M2 channel computed real and complex Cepstrum and estimated the minimum phase impulse response. (a) Sleep stage W. (b) Sleep stage R.

D. Cepstral statistics

The use of cepstral statistics for sleep stage classification offers several advantages, including reduced reliance on manual annotations and improved consistency in stage labeling. Additionally, the interpretability of cepstral features allows for better insights into the underlying EEG characteristics associated with different sleep stages. Future research can explore the application of advanced machine learning techniques, such as deep learning, in conjunction with cepstral features to further enhance sleep stage classification performance. In this paper, we present a novel approach for sleep stage classification based on cepstral analysis. We compute cepstrum statistics, including mean value, variance, skewness, kurtosis, and entropy, from EEGs, EOGs, EMG and ECG signals to extract discriminative features for sleep stage classification. Our study demonstrates the effectiveness of cepstral statistics in improving the accuracy and reliability of sleep stage classification compared to traditional methods, providing a promising avenue for sleep research and diagnostics.Moreover, the generated cepstral statistics functioned as identifiable characteristics for machine learning classifiers.

Continue, we describe the statistical measures where used. The mean value of the cepstrum provides insights into the central tendency of the spectral characteristics. It is computed

as the average of the cepstral coefficients over a specified window or frame. Mathematically, Mean determined as

$$E[C_x] = (1/N) \cdot \sum_{i=1}^{N} C_x(i)$$

where N is the number of cepstral coefficients and i ranges from 1 to N.

Variance quantifies the spread or dispersion of cepstral coefficients. It is computed as

$$Var[C_x] = (1/N) \cdot \sum_{i=1}^{N} (C_x(i) - E[C_x])^2$$

Kurtosis characterizes the peakedness or flatness of the cepstrum distribution. High kurtosis indicates a sharper peak. Kurtosis

$$K[C_x] = (1/N) \cdot \sum_{i=1}^{N} \left(\frac{(C_x(i) - E[C_x])}{Var[C_x]} \right)^4$$

Entropy measures the information content or disorder in the cepstrum coefficients. It is computed as

$$I[C_x] = -\sum_{i=1}^{N} (C_x(i) \cdot \log(C_x(i)))$$

where the sum is taken over all cepstral coefficients.

E. Bicepstral analysis

To conduct a more thorough study of the data, we conducted bicepstral analysis on all channels in the same manner as cepstral analysis. Once again, the EOG_E1_M2 channel produced the most important findings. By looking at the calculated bicepstrum values in 2D space, we hope to distinguish between the various stages of sleep. The average values of all collected patient data are first derived, and utilizing these values, the FFT technique is used to estimate the bicepstrum. To notice any changes in a more thorough study, we thus introduced partitioning in the data vector in a similar way as we did in the cepstral analysis. In Fig.2 (a) depicted the calculated bicepstrum for the weak sleep stage and in (b) for the REM sleep stage. We observe that for the REM stage the bicepstrum diagram is much denser than the weak stage case in the whole quefrency region. Also, for the REM situation, it tends to exhibit values with greater amplitude which suggests that for this sleep stage the noninear phenomena are more intense. From these illustrations of bicepstrum (a),(b) the difference between the two stages of sleep becomes clear and we can use these calculations to classify them.

F. Bicepstral statistics

Using the computed bicepstral coefficients by the methodology described previously , we conduct a more extensive analysis by calculating statistical measures for sleep stage classification. For our purpose , we can observe in Figures 2 that for the channels EEG_C4_M1 and EEG_O2_M1 the distribution of computed values of entropy differs between distinct sleep stages. Also, this result is reflected in Fig.3 (a),(b),(c)

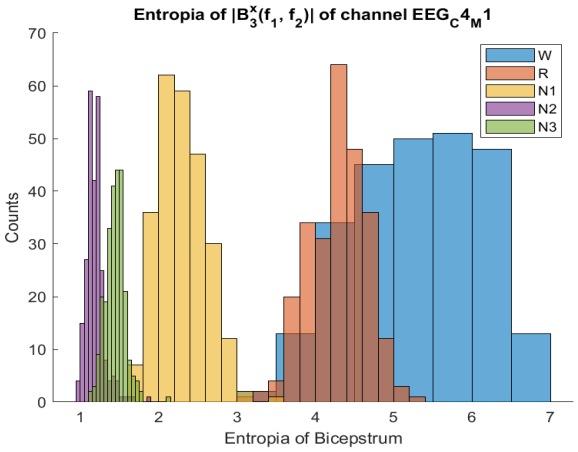

(a) Entropy of EEG_C4_M1 channel

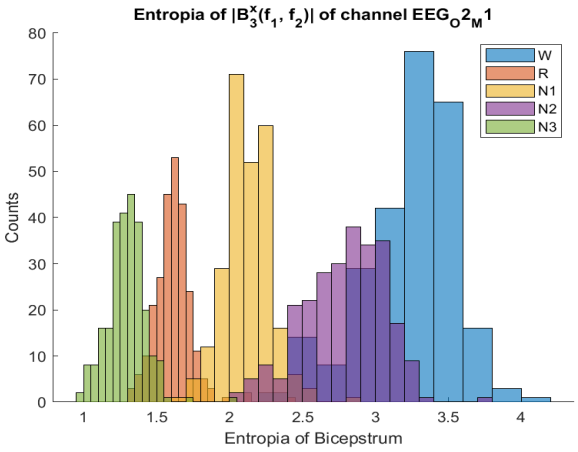

(b) Entropy of EEG_O2_M1 channel

Fig. 2: Entropy of EEGs channels on computed bicepstrum

where the distribution of variance values for the channels (a) EEG_C4_M1, (b) EEG_O2_M1 and (c) EMG_chin is examined . Moreover ,this result might be inferred from the histograms of the distribution of entropy and squared entropy measures. From this illustrations , it is obvious that we have the possibility to distinguish the separate sleep stages for a patient by executing bicepstral analyis and computing the statistical measures over that.

G. Bicoherence

Our last attempt focused on using the higher order statistics of the PSG recordings in order to extract features that can be used for the classification of the sleep stage. More specifically, for every patient, channel and epoch the bicohereney was estimated using the direct method, with $K = 32$ segments and $f_c = 64Hz$ cut-off frequency resulting in a unique "*frame*". Figure 5 shows the bicoherence in two different frames.

1) Feature Extraction: Following the estimation of a every frame, a number of features where calculated. These include

- Mean, m
- Standard Deviation, s
- Skewness, g.

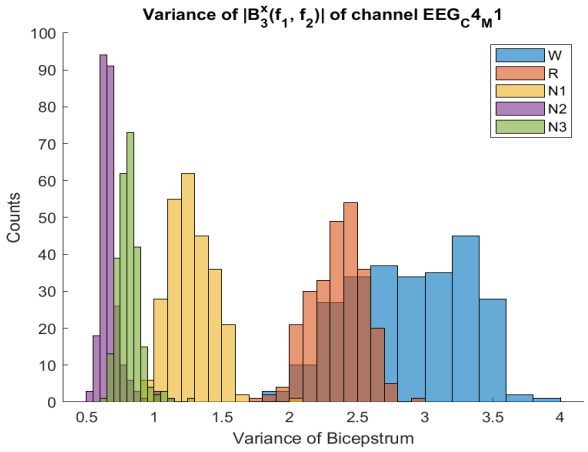

(a) Variance of EEG_C4_M1 channel

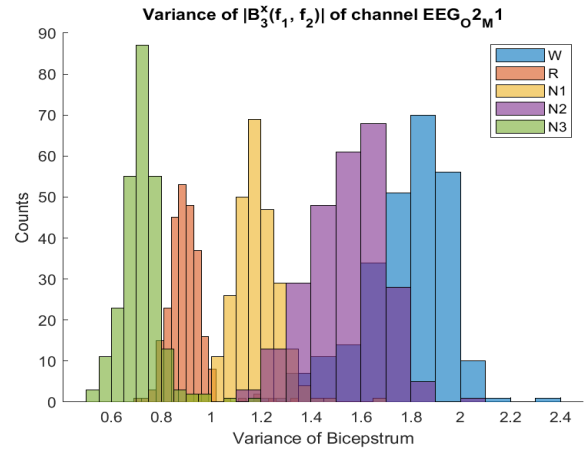

(b) Variance of EEG_O2_M1 channel

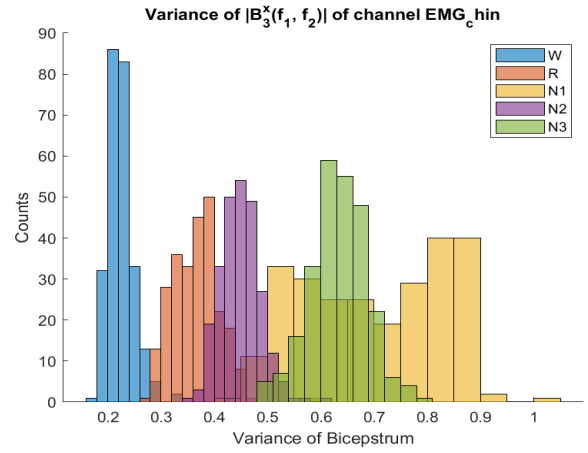

(c) Variance of EMG_chin channel

Fig. 3: Variance of EEGs and EMG channels on computed bicepstrum

- Entropy, $h = \mathbb{E}_{X\sim bic}[-log_2 X]$.
- Square Root entropy, $\sqrt{h} = \mathbb{E}_{X\sim\sqrt{bic}}[-log_2 X]$.

In table I is presented a sample of the features that where calculated.

We also used the bicoherence to examine the presence of Quadratic Phase Cupling (QPC) in the recordings. The

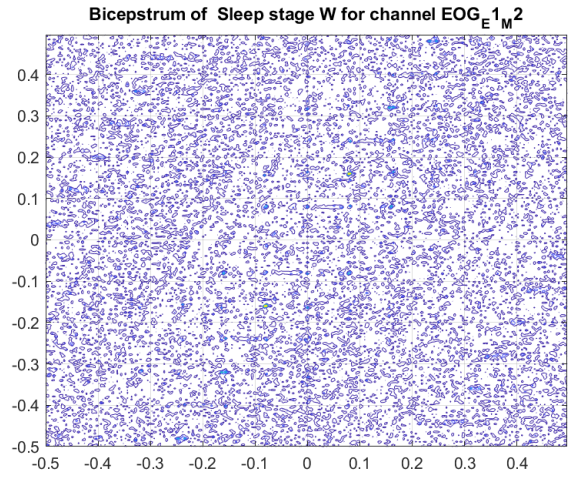

(a) Sleep stage: Weak

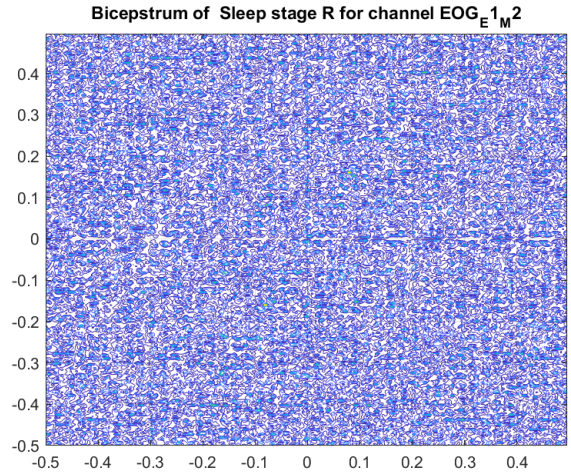

(b) Sleep stage: REM

Fig. 4: EOG_E1_M2 channel

following approach was used. First we used a peak finding algorithm to detect the peaks in every frame. Figure 6 displays the result of the peak finding algorithm when applied to a frame. In a similar way as before a number of features where calculated from the set of peaks that was found. If the set of found peaks is $P = \{(x_i, y_i) \in PR\}_{i=1}^{N}$ the we computed the following features:

- number of peaks, N.
- Mean value of peaks,

$$\bar{P} = \frac{1}{N} \sum_{(x,y)\in P} bic(x, y)$$

.

- Mean x-value,

$$\bar{P}^{(x)} = \frac{1}{N} \sum_{i=1}^{N} x_i$$

.

- Mean y-value,

$$\bar{P}^{(y)} = \frac{1}{N} \sum_{i=1}^{N} y_i$$

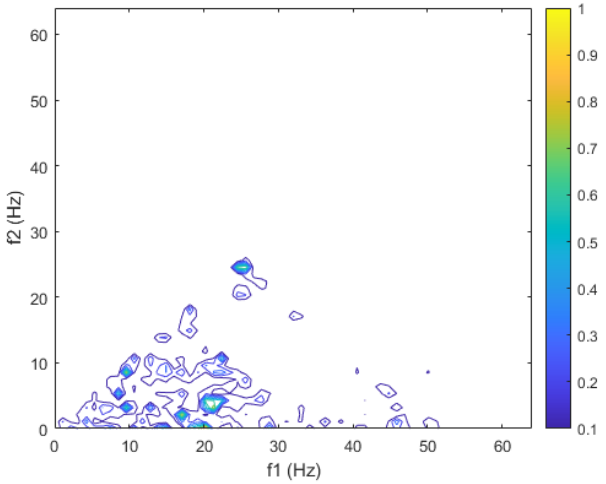

(a) Bicoherence during Wake stage

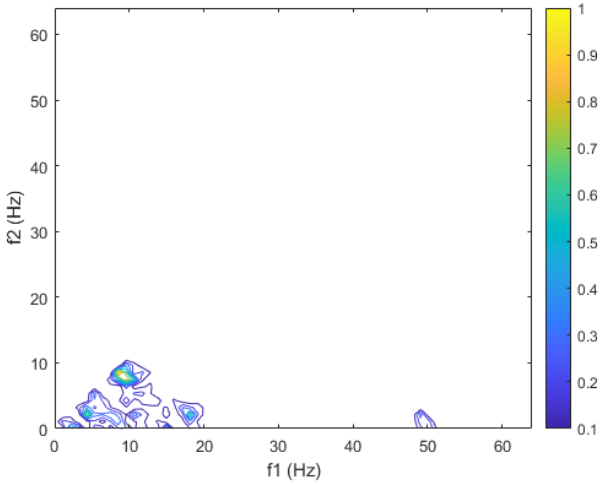

(b) Bicoherence during stage N3

Fig. 5: Bicoherence estimated from the recording of patient SN001 during the 1st epoch (a) and 112th epoch (b).

.

channel	mean	std	skewness	entr	sqrt_entr	Stage
6	0.00699	0.05380	12.29121	0.82117	0.82063	N2
6	0.00995	0.05817	8.97416	1.07092	1.06951	N1
5	0.01112	0.05751	8.54181	1.36140	1.36066	N2
5	0.01507	0.07276	7.66069	1.71473	1.71109	W
6	0.00466	0.03826	14.19907	0.67745	0.67691	N2
3	0.01596	0.07503	7.51376	1.60890	1.60783	N1

TABLE I: Table of features extracted from patient SN001.

2) Machine Learning Model: Having in our hands a vector $\mathbf{F^{(i)}}$ of features for every frame i we applied PCA in order to use only the coordinates with the most information. Subsequently we trained a *k-nearest neighbors* model using the PCA features in order to classify the sleep stage.

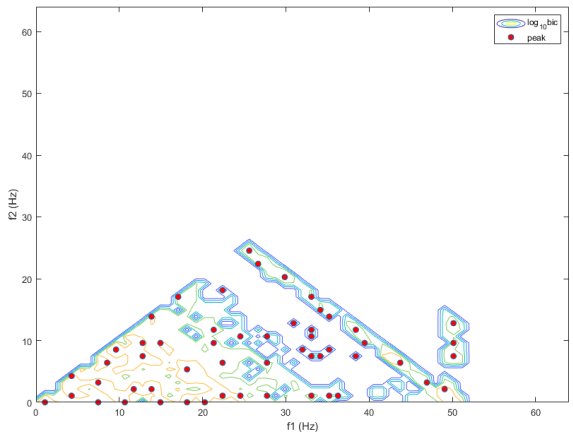

Fig. 6: Peaks that were found from the peak finding algorithm for patient SN010, epoch 231 and channel EEG F4/M1.

IV. Results and Review

A. Feature Extraction

Figure 7 presents the distribution of some of the features when computed on the whole deadset and condition on the sleep stage. It is evident from just observing the histograms that there is a significant difference in the distribution of the features among the different stages. In particular, the differences among stages W, N3 and R are the most noticeable. Therefore, we expect that a model trained on these features will do a better job at differentiating among these three stages and will make mistakes on the remaining two stages.

B. PCA

In order for the classification algorithm to have good performance we applied Principal Component Analysis and reduced the dimensions of the feature vectors. Figure 8 displays the eigenvalues of the covariance matrix. We can see that after the 4th principal component the contribution of information becomes negligible. Therefore we kept up to the 4th principal component, meaning that the resulting data point belong to 4-dimensional euclidean space.

C. k-Nearest Neighbors classification process

First off, the chosen dataset is not at all balanced, contrary to what the literature suggests. To be specific we have 23519 W, 15415 N1, 49256 N2, 26407 N3 and 20963 REM 30s epochs out of a total of 135560 (not including subjects 14,18,36,64,98 and 120 due to corrupted ECG). Consequently, using basic accuracy as our main criterion would be inaccurate. Cohen's kappa [31] is a more appropriate statistic that is frequently employed in automatic sleep stage score evaluation [7], [28], [29], and [30]. Instead of focusing on simple accuracy, Cohen's kappa measures inter-rater agreement and eliminates the potential of agreement by coincidence.

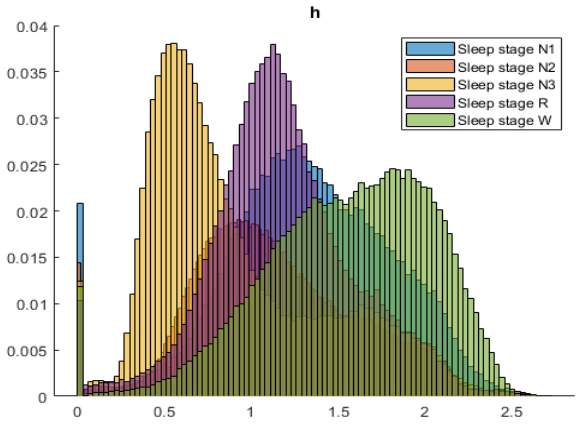

(a) Entropy h.

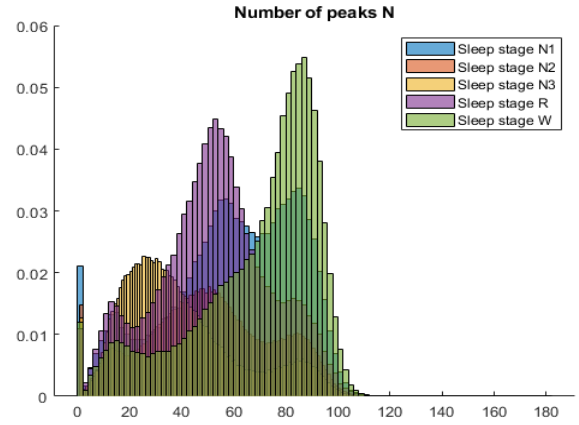

(b) Number of peaks N

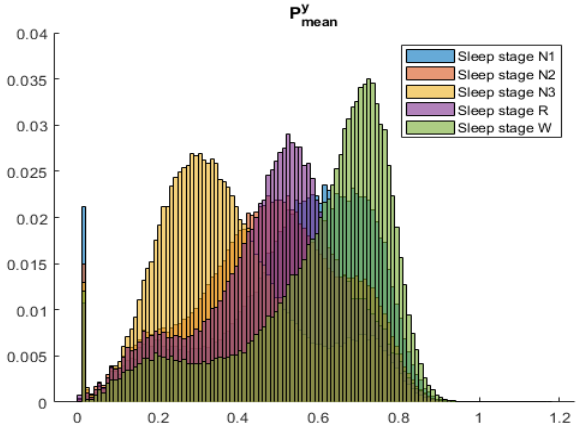

(c) mean y-value

Fig. 7: Histogram of entropy (a), number of peaks found (b) and $\bar{P}^{(y)}$ (c), categorized by epoch

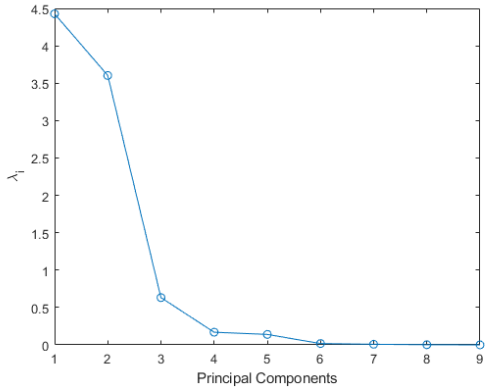

Fig. 8: Principal component variances, that is the eigenvalues of the covariance matrix of the features.

A k-Nearest Neighbors (kNN) classifier was trained to classify the sleep stage based on the observed feature vector. The model was tuned to use the Spearman Distance and with $k = 16$ neighbors. The model was trained on the 70% of the dataset, the remaining of which was left for testing and validation. The results are shown in figure 9.

The model's confusion matrix is shown in Figure 9, and from it we may determine where the model is lacking. We can see that the classification is minimal to nonexistent, or even random. Both the classification optimization approach and the weak EOG and EMG characteristics are to blame for these errors. None of the suggested classifiers make use of temporal data in any way. The fact that humans experience numerous cycles of non-REM and REM stages when they sleep makes this the fundamental flaw in our prediction models. We also noticed that our classifiers struggled to distinguish between waking and REM sleep. This is because those stages show relatively comparable EEG activity, making the only trustworthy method of differentiating between those two classes to rely on the EOG patterns. Sadly, the useful EOG data is not well captured by our suggested feature-set. Last but not least, the lack of information regarding the pathologies of the dataset's participants has a negative impact on the performance of the classifiers.

A suggested course of action would be to apply additional EOG analysis and make use of some cutting-edge features that have been described in literature, such as [32], to categorize eye movements as slow or quick. Further EMG analysis is also advised. At first glance, improved low frequency filtering would be beneficial. Even some conventional EEG parameters that were disregarded in this investigation, including sub-band relative energy, may turn out to be helpful.

V. Conclusion

As a conclusion, this research suggests an automated sleep stage categorization based on a combination of machine learning and signal processing techniques. A comprehensive feature-set was created, in particular, by using HOS and cepstral-bicepstral analysis on PSG recording signals. The classification performance using KNN-method provides relevant information about some of the characteristics. It seems

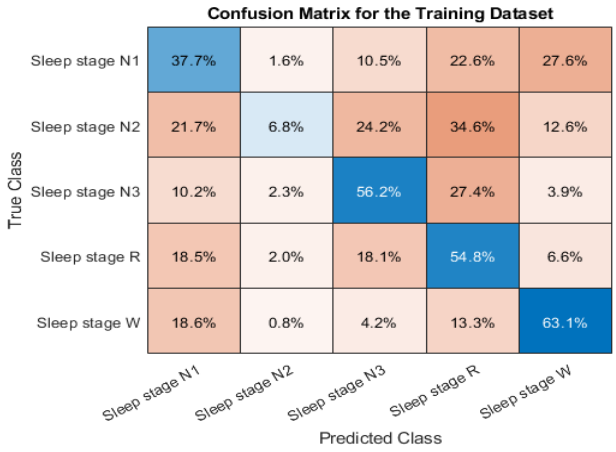

(a) Training Dataset.

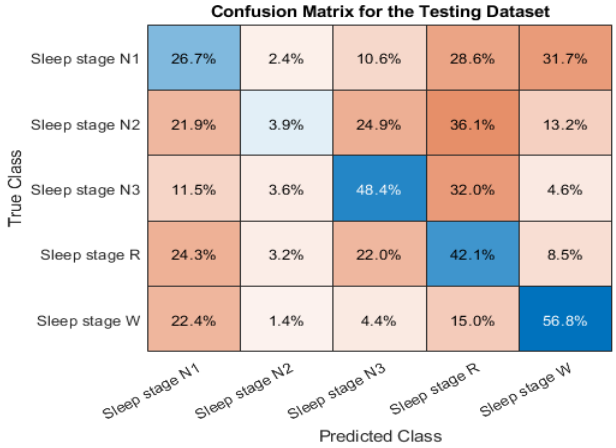

(b) Testing Dataset

Fig. 9: Confusion matrix of the kNN model in training (a) and testing (b) datasets.

that further research is necessary, either to fine-tune the classification algorithm .

VI. Code implementation

The code for the given analysis can be found at this public repository: https://github.com/alextsigilis/ptes.git

References

[1] M. Aminoff, F. Boller, and D. Swaab, "We spend about one-third of our life either sleeping or attempting to do so," *Handbook of clinical neurology / edited by P.J. Vinken and G.W. Bruyn*, vol. 98, p. vii, 01 2011.

[2] S. Chokroverty et al., "Overview of sleep & sleep disorders," *Indian J Med Res*, vol. 131, no. 2, pp. 126–140, 2010.

[3] T. J. Sejnowski and A. Destexhe, "Why do we sleep?" *Brain research*, vol. 886, no. 1-2, pp. 208–223, 2000.

[4] R. B. Berry, R. Brooks, C. Gamaldo, S. M. Harding, R. M. Lloyd, S. F. Quan, M. T. Troester, and B. V. Vaughn, "Aasm scoring manual updates for 2017 (version 2.4)," pp. 665–666, 2017.

[5] A. K. Patel, V. Reddy, and J. F. Araujo, "Physiology, sleep stages," in *StatPearls [Internet]*. StatPearls Publishing, 2021.

[6] M. A. Carskadon, W. C. Dement et al., "Normal human sleep: an overview," *Principles and practice of sleep medicine*, vol. 4, no. 1, pp. 13–23, 2005.

[7] D. Alvarez-Estevez and R. M. Rijsman, "Inter-database validation of a deep learning approach for automatic sleep scoring," *PloS one*, vol. 16, no. 8, p. e0256111, 2021.

[8] M. Sharma, A. Yadav, J. Tiwari, M. Karabatak, O. Yildirim, and U. R. Acharya, "An automated wavelet-based sleep scoring model using eeg, emg, and eog signals with more than 8000 subjects," *International Journal of Environmental Research and Public Health*, vol. 19, no. 12, p. 7176, 2022.

[9] B. P. Lucey, J. S. Mcleland, C. D. Toedebusch, J. Boyd, J. C. Morris, E. C. Landsness, K. Yamada, and D. M. Holtzman, "Comparison of a single-channel eeg sleep study to polysomnography," *Journal of sleep research*, vol. 25, no. 6, pp. 625–635, 2016.

[10] D. L. Donoho, S. G. Mallat, R. von Sachs et al., "Estimating covariances of locally stationary processes: rates of convergence of best basis methods," Departement of Statistics, Stanford University, Tech. Rep., 1998.

[11] D. P. Subha, P. K. Joseph, R. Acharya U, C. M. Lim et al., "Eeg signal analysis: a survey," *Journal of medical systems*, vol. 34, no. 2, pp. 195–212, 2010.

[12] N. Arthur and J. Penman, "Induction machine condition monitoring with higher order spectra," *IEEE Transactions on Industrial Electronics*, vol. 47, no. 5, pp. 1031–1041, 2000.

[13] C. Courtney, S. Neild, P. Wilcox, and B. Drinkwater, "Application of the bispectrum for detection of small nonlinearities excited sinusoidally," *Journal of Sound and Vibration*, vol. 329, no. 20, pp. 4279–4293, 2010.

[14] A. J. Hillis, S. A. Neild, B. W. Drinkwater, and P. D. Wilcox, "Global crack detection using bispectral analysis," *Proceedings of the Royal Society A: Mathematical, Physical and Engineering Sciences*, vol. 462, no. 2069, pp. 1515–1530, 2006.

[15] W. Collis, P. White, and J. Hammond, "Higher-order spectra: the bispectrum and trispectrum," *Mechanical systems and signal processing*, vol. 12, no. 3, pp. 375–394, 1998.

[16] Nikias, C.L. and M.R. Raghuveer, "Bispectrum estimation: A digital signal processing framework," *Proc. IEEE*, Vol. 75, pp. 869-91, July 1987.

[17] R. Makhijani, U. Shrawankar, and V. M. Thakare, "Speech enhancement using pitch detection approach for noisy environment," arXiv preprint arXiv:1305.2352, 2013.

[18] A. V. Oppenheim and R. W. Schafer, "From frequency to quefrency: A history of the cepstrum," *IEEE signal processing Magazine*, vol. 21, no. 5, pp. 95–106, 2004.

[19] A. L. Goldberger, L. A. N. Amaral, L. Glass, J. M. Hausdorff, P. C. Ivanov, R. G. Mark, J. E. Mietus, G. B. Moody, C.-K. Peng, and H. E. Stanley, "PhysioBank, PhysioToolkit, and PhysioNet: Components of a new research resource for complex physiologic signals," *Circulation*, vol. 101, no. 23, pp. e215–e220, 2000 (June 13), circulation Electronic Pages: http://circ.ahajournals.org/content/101/23/e215.full PMID:1085218; doi: 10.1161/01.CIR.101.23.e215.

[20] S. Mart´ın-Gonzalez, J. L. Navarro-Mesa, G. Juli ´ a-Serd ´ a, J. F. Kraemer, ´ N. Wessel, and A. G. Ravelo-Garc´ıa, "Heart rate variability feature selection in the presence of sleep apnea: An expert system for the characterization and detection of the disorder," *Computers in biology and medicine*, vol. 91, pp. 47–58, 2017.

[21] F. Shaffer and J. P. Ginsberg, "An overview of heart rate variability metrics and norms," *Frontiers in public health*, p. 258, 2017.

[22] R. Singh, R. Mehta, and N. Rajpal, "Efficient wavelet families for ecg classification using neural classifiers," *Procedia computer science*, vol. 132, pp. 11–21, 2018.

[23] J. Pan and W. J. Tompkins, "A real-time qrs detection algorithm," *IEEE transactions on biomedical engineering*, no. 3, pp. 230–236, 1985.

[24] H. Sedghamiz, "Matlab implementation of pan tompkins ecg qrs detector," Code Available at the File Exchange Site of *MathWorks*, 2014.

[25] R. Yan, F. Li, X. Wang, T. Ristaniemi, and F. Cong, "An automatic sleep scoring toolbox: multi-modality of polysomnography signals' processing," in *International Conference on Signal Processing and Multimedia Applications*. SCITEPRESS Science And Technology Publications, 2019.

[26] C.-E. Kuo, S.-F. Liang, Y.-C. Lee, F.-Y. Cherng, W.-C. Lin, P.-Y. Chen, Y.-C. Liu, and F.-Z. Shaw, "An eog-based automatic sleep scoring system and its related application in sleep environmental control," in *International Conference on Physiological Computing Systems*. Springer, 2014, pp. 71–88.

[27] Y. Freung and R. Shapire, "A decision-theoretic generalization of online learning and an application to boosting," *J Comput Syst* Sci, vol. 55, pp. 119–139, 1997.

[28] H. Danker-hopfe, P. Anderer, J. Zeitlhofer, M. Boeck, H. Dorn, G. Gruber, E. Heller, E. Loretz, D. Moser, S. Parapatics et al., "Interrater reliability for sleep scoring according to the rechtschaffen & kales and the new aasm standard," *Journal of sleep research*, vol. 18, no. 1, pp. 74–84, 2009.

[29] U. J. Magalang, N.-H. Chen, P. A. Cistulli, A. C. Fedson, T. G´ıslason, D. Hillman, T. Penzel, R. Tamisier, S. Tufik, G. Phillips et al., "Agreement in the scoring of respiratory events and sleep among international sleep centers," *Sleep*, vol. 36, no. 4, pp. 591–596, 2013.

[30] M. L. McHugh, "Interrater reliability: the kappa statistic," *Biochemia medica*, vol. 22, no. 3, pp. 276–282, 2012.

[31] J. Cohen, "A coefficient of agreement for nominal scales," *Educational and psychological measurement*, vol. 20, no. 1, pp. 37–46, 1960.

[32] D. Alvarez-Estevez, I. van Velzen, T. Ottolini-Capellen, and B. Kemp, "Derivation and modeling of two new features for the characterization of rapid and slow eye movements in electrooculographic sleep recordings," *Biomedical Signal Processing and Control*, vol. 35, pp. 87–99, 2017.

[33] Jolliffe, lan T. Cadima, "Principal component analysis: a review and recent developments" . *Philosophical Transactions of the Roval* Society A: Mathematical. Physical and Enqineering Sciences. 374

[34] Abdi. H. & Williams, L.J. (2010). "Principal component analysis". *Wiley Interdisciplinary Reviews: Computational Statistics*. 2 (4): 433-459.

[35] Jolliffe, I. T. (2002). Principal Component Analysis Z. *Springer Series in Statistics*. New York: Springer-Verlag.

[36] Cover, Thomas M.; Hart, Peter E. (1967). "Nearest neighbor pattern classification" . *IEEE Transactions on Information Theory*. 13 (1):21–27.

[37] Coomans, Danny; Massart, Desire L. (1982). "Alternative k-nearest neighbour rules in supervised pattern recognition : Part 1. k-Nearest neighbour classification by using alternative voting rules". *Analytica Chimica Acta*. 136: 15-27.

[38] Hall, Peter; Park, Byeong U.; Samworth, Richard J. (2008). "Choice of neighbor order in nearest-neighbor classification". *Annals of Statistics*. 36 (5): 2135-2152.